PROCEEDINGS OF SCIENCE

Overview of the current status for the search of electroweak bosons in CMS

Saptaparna Bhattacharya*
Northwestern University
E-mail: saptaparna.bhattacharya@northwestern.edu

With the collection of more than 150 fb^{-1} of data in Run I and Run II of the Large Hadron Collider, precision tests of the Standard Model (SM) are becoming increasingly possible. We present the current status of diboson searches, where the production mechanisms involve both quark-antiquark annihilation and vector boson scattering (VBS). Cross sections of diboson processes such as WW and WZ have been measured with high precision. The study of these processes is crucial in raising the sensitivity of Higgs physics where they feature as backgrounds. In addition to the inclusive cross sections, differential cross sections parametrized as a function of the transverse momentum of the bosons have been measured. For production modes through VBS, the precision of the measurements are limited by the statistics of the datasets. The search for rare SM processes such as, triboson production and double parton scattering is also presented. The discovery potential of some of these processes is augmented by the use of advanced multivariate techniques. A summary of the current status of the measurement of anomalous trilinear and quartic couplings is also presented.

ALPS 2019 An Alpine LHC Physics Summit
April 22 - 27, 2019
Obergurgl, Austria

*Speaker.

PoS(ALPS2019)055

1. Introduction

The discovery of the Higgs boson in 2012 and the subsequent measurements of its width and couplings to quarks and leptons has placed the Standard Model of Particle Physics (SM) on strong footing. The large amount data collected at the Large Hadron Collider (LHC) over the course of Run I and II allow us to perform precision tests of the SM. These measurements of the SM processes can be used to place indirect constraints on new physics. The search for dibosons and tribosons offer probes of the non-Abelian $SU(2) \times U(1)$ gauge symmetry of the SM. This note is structured as follows. In Sec. 2, the status of diboson searches performed with the Compact Muon Solenoid (CMS) detector is discussed with an emphasis on the precision of the cross section measurements, which are entirely driven by experimental and theoretical systematic uncertainties. In Sec. 3, the discovery of the Vector Boson Scattering (VBS) processes is discussed. In Sec. 4, rare processes such as the search for triboson processes and double parton scattering is discussed and finally in Sec. 5, the current status of the search for anomalous trilinear and quartic couplings is summarized.

2. Search for diboson production

The production of diboson processes in the SM occurs through the s, t and u-channel Feynman diagrams as shown in Fig. 1. The s-channel diagram with the ZZZ vertex is forbidden in the SM and can only occur if anomalous contributions to the SM exist. In addition to these diagrams, the contribution from subdominant processes such as $gg \to VV$ to the total production cross section is also taken into account.

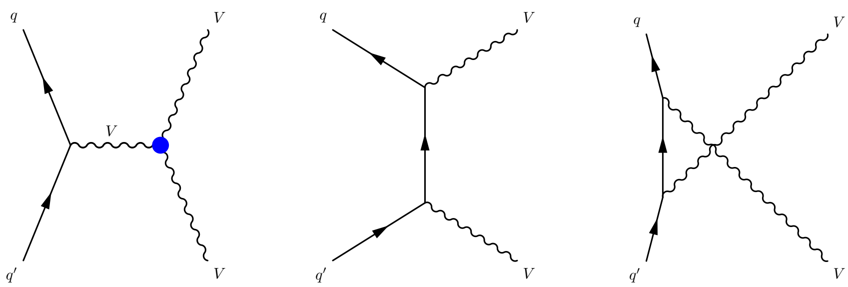

Figure 1: The s, t and u channel Feynman diagrams pertaining to diboson production. The s channel diagram exists only in the case of the WW and WZ production. In the case of ZZ production, the vertex shown in blue exists only if the SM acquires anomalous contributions.

2.1 Search for WW

The search for WW production [1] is carried out in the fully leptonic decay channel, specifically electron-muon, in order to reduce the deleterious effects of the Drell-Yan background. Two isolated leptons are selected and any top-quark mediated backgrounds are suppressed by vetoing bottom-quarks jets (b-jets). To be sensitive to the missing transverse energy ($\vec{E}_{\mathrm{T}}^{\mathrm{miss}}$) arising from the presence of neutrinos in the final state, any missing transverse energy ($\vec{E}_{\mathrm{T}}^{\mathrm{miss}}$) originating from the mismeasurement of lepton momenta is reduced through requirements on azimuthal correlations between the $\vec{E}_{\mathrm{T}}^{\mathrm{miss}}$ and the lepton momenta. The WW cross section is computed in both 0-jet and

1-jet categories. The $\vec{E}_T^{\text{miss}}$ spectra in the 0-jet category in shown in Fig. 2. The Higgs $\rightarrow WW$ process is assumed to be a background in this search.

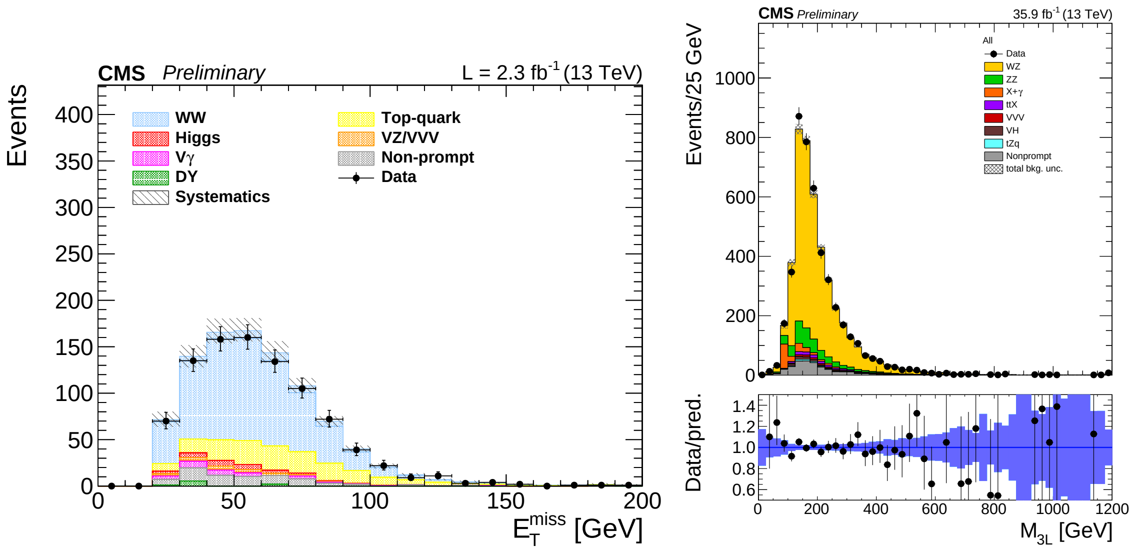

Figure 2: The missing transverse energy (MET) in a two lepton selection in 0-jet category (left) and the invariant mass of the three-lepton system in the WZ signal region (right).

The combined cross section obtained is:
$\sigma(\mathbf{pp} \rightarrow \mathbf{W^+W^-}) = \mathbf{115.5} \pm \mathbf{5.8}$ (stat.) $\pm\, \mathbf{5.8}$ (exp. syst.) $\pm\, \mathbf{6.4}$ (theo. syst.) $\pm\, \mathbf{3.6}$ (lumi.) pb
The largest sources of experimental uncertainty (4.9%) are associated with lepton and b-jet identification. The subdominant uncertainty (3.2%) is from factorization and renormalization scales and two different event generators (POWHEG [2] and HERWIG++ [3]) are used to ascertain hadronization and underlying event uncertainties. While this search uses a small fraction of the total data collected, it should be noted that the measurement is dominated by systematic uncertainties. Uncertainties associated with b-jet identification are expected to be lower with the analysis of the full dataset collected by CMS.

2.2 Search for WZ

The search for WZ production [4] is performed in a trilepton channel where the three leptons arise from the fully leptonic decay of both the W and the Z bosons. At least one opposite-sign and same-flavor lepton pair is required and the invariant mass of the trilepton system (shown on the right panel of Fig. 2) is required to be greater than 100 GeV to mitigate the effect of fake leptons. Since there is no real b-jet in the final state, a b-jet veto is imposed and any additional fourth lepton is rejected to reduce the ZZ background. This analysis represents the most precise, by a factor of two, measurement of the WZ cross section.

The combined fiducial cross section in four lepton flavor based channels is computed for events with at least one pair of opposite-sign same flavor (OSSF) leptons, where the invariant mass of the OSSF lepton is required to lie between 60 and 120 GeV. The combined cross section obtained is:
$\sigma(\mathbf{pp} \rightarrow \mathbf{WZ}) = \mathbf{257.5} \pm \mathbf{5.2}$ (stat.) $\pm\, \mathbf{12.2}$ (exp. syst.) $\pm\, \mathbf{2.2}$ (theo. syst.) $\pm\, \mathbf{7.4}$ (lumi.) fb

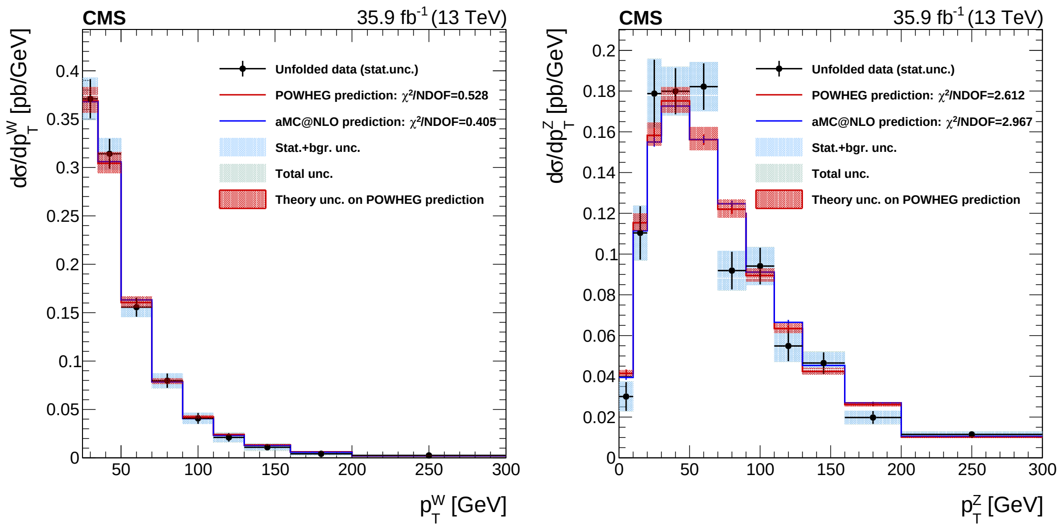

Figure 3: The differential distribution of the transverse momentum of the W^+ (left) and Z boson (right).

As in the case of the W^+W^- cross section, the final measurement in this case is limited by systematic uncertainties, the largest of which is related to the lepton identification uncertainty and the b-tagging uncertainty. The theoretical uncertainties associated with factorization and renormalization scales account for 0.9% of the total uncertainty. The WZ process offers the possibility of measuring differential cross sections as a function of the vector boson p_T as shown in Fig. 3. The tails of such distributions are expected to acquire enhancements if anomalous couplings exist. The agreement between data and simulation is within statistical uncertainties implying that these sensitive variables are well modeled in simulations. The WZ process can also be used to measure the ratio of the cross section of the positive and negatively charged W boson production. The quantity, $\frac{pp \to W^+Z}{pp \to W^-Z}$ = 1.48 $\pm$ 0.06, is one of the most precisely measured ratios with an error of $\sim$4%.

2.3 Search for ZZ

The search for ZZ production [5] is performed in a four-lepton final state, where the dominant mode of ZZ production is the t-channel diagram as shown in Fig. 1. A subdominant mode, that accounts for 10% of the total production cross section is through the $gg \to ZZ$ diagram. The four-lepton channel provides a clean topology for discovery, as is evident in Fig. 4, where the signal purity is greater than 90%. The fiducial cross section is computed for a case where the invariant mass of the two Z-boson candidates in the event is required to lie between 60 - 120 GeV. The largest source of uncertainty in the cross section arises from the lepton identification uncertainty.

The fiducial cross section combined for all three years for data-taking (2016-2018) obtained is: $\sigma(\mathbf{pp} \to \mathbf{ZZ}) = \mathbf{39.9} \pm \mathbf{0.7}\ (\mathrm{stat.}) \pm \mathbf{1.0}\ (\mathrm{exp.\ syst.}) \pm \mathbf{0.7}\ (\mathrm{lumi.})$ fb

This represents the most precise determination of the ZZ production cross section. The measurement of the cross section of this process, along with the theoretical predictions, across several center of mass energies is shown in the right panel of Fig. 4.

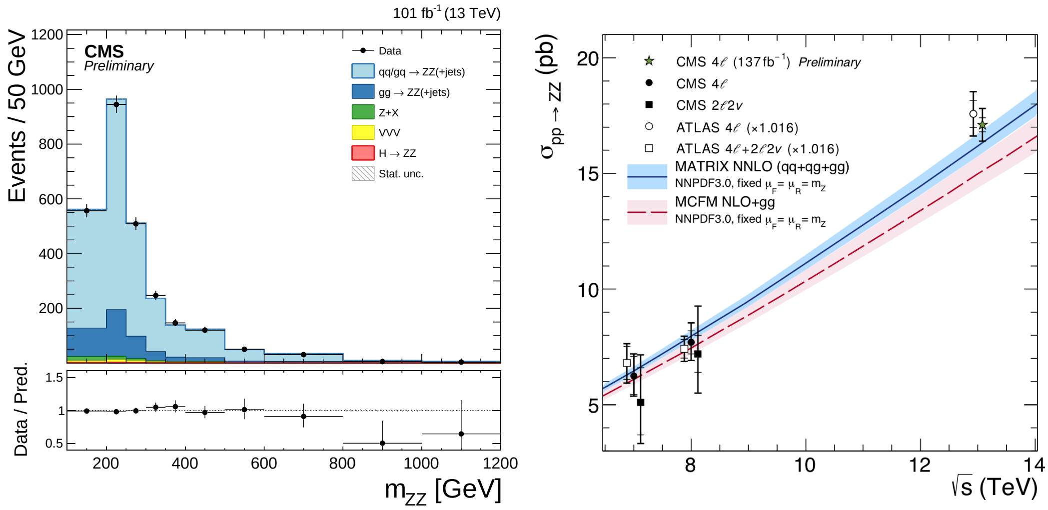

Figure 4: Left panel: The invariant mass of the ZZ where the production modes are separated into quark-induced or quark-gluon induced (light blue) and purely gluon induced (dark blue). Right panel: Summary of the ZZ cross section measurements across several center of mass energies ($\sqrt{s}$).

3. Vector boson scattering

The vector boson scattering topology consists of two jets and two identically charged leptons (shown on the left panel of Fig. 5). The production and decay modes of WW through the VBS mechanism is shown in the Feynman diagram on the right panel of Fig. 5. Owing to the lack of color flow in the event, there is a "rapidity gap" between the jets and the leptons, which can be exploited by making optimized requirements on the Zeppenfeld variable, defined as, $z_l^* = |\eta_l - \frac{1}{2}(\eta_{j1} - \eta_{j2})|/|\Delta\eta_{jj}|$ where l and j refer to the lepton and the jet respectively with 1 and 2 being the indices of the two jets. The Zeppenfeld variable is computed for each of the leptons and its definition is augmented based on the complexity of the final state. Since the jets carry a major fraction of the momenta of the initial state quarks, they are highly energetic. For the computation of the fiducial cross section, the mass of these jets (M_{jj}) is required to be greater than 500 GeV.

3.1 Search for VBS WW

The search for VBS WW production [6] is carried out in a same-sign dilepton final state, where the VBS topology is targetted by requiring that the invariant mass of the two highest p_T jets (M_{jj}, shown on the left panel of Fig. 6) is greater than 500 GeV. The production of identically charged WW pairs, through the VBS topology is observed with a significance of 5.5 σ. The fiducial cross section for VBS WW is computed for $M_{jj} > 500$ GeV (shown in Fig. 6) and $|\eta| > 2.5$ and is measured to be:

$$\sigma(\mathbf{pp} \to \mathbf{WW}(\mathbf{VBS})) = \mathbf{3.83} \pm \mathbf{0.66}\ (\text{stat.}) \pm \mathbf{0.35}\ (\text{exp. syst.})\ \text{fb}$$

The distribution of the invariant mass of the two leptons (M_{ll}, shown on the right panel of Fig. 6) can be used to explore new physics scenarios specifically in the context of anomalous contributions to the SM.

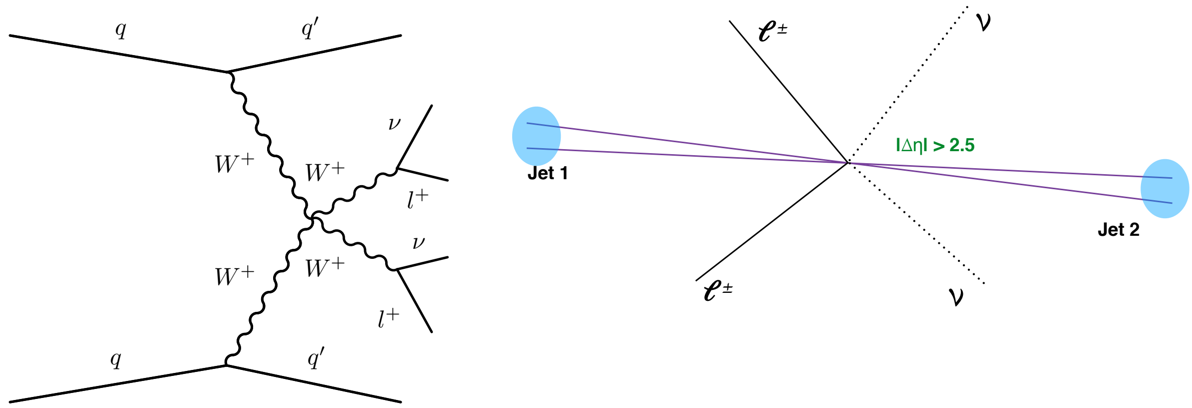

Figure 5: Left panel: The production of same-signed WW in association with two jets through vector boson scattering (VBS). Right panel: The description of the VBS topology through its signature in the CMS detector. The event is characterized by the presence of two high p_T jets and central bosons.

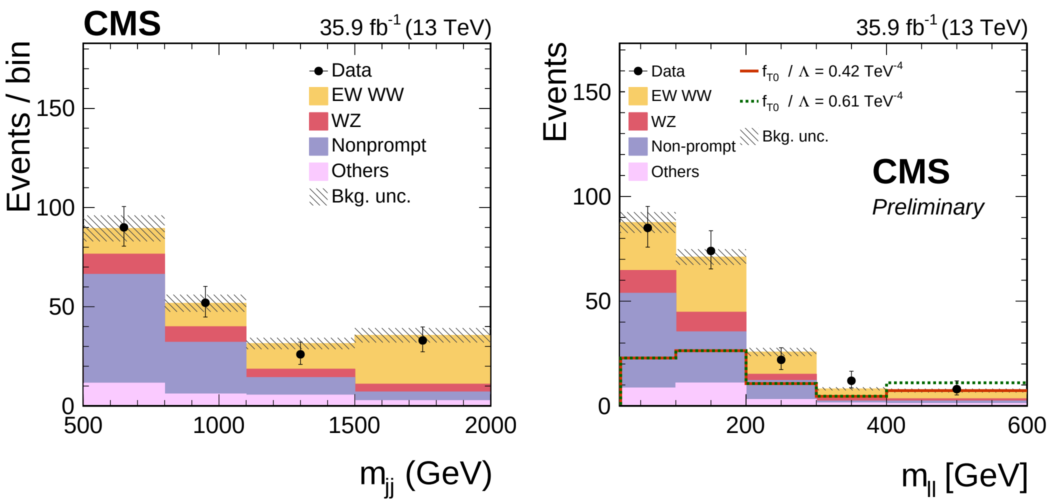

Figure 6: Left panel: The invariant mass of the two highest p_T jets in a VBS WW event. Right panel: The invariant mass of the leptons in a VBS WW event. This spectra can be used to explore new physics scenarios.

3.2 Search for VBS WZ

The search for VBS WZ [7] is performed in a final state characterized by the presence of exactly three leptons. In this case, the Zeppenfeld variable is modified as: $\eta^*_{3l} = \eta_{3l} - \frac{1}{2}(\eta_{j1} + \eta_{j2})$ and is required to lie between $\pm$ 2.5. The largest source of background for the electroweak production of WZ is the QCD induced production of the identical process. To reduce the QCD induced contribution, the distribution of the invariant mass of the two highest p_T jets (shown on the left panel of Fig. 7) and the rapidity separation between these jets (shown on the right panel of

Fig. 7) is profiled on a 2D plane as the ratio of the electroweak to the QCD induced production of the WZ increases as a function of these two variables.

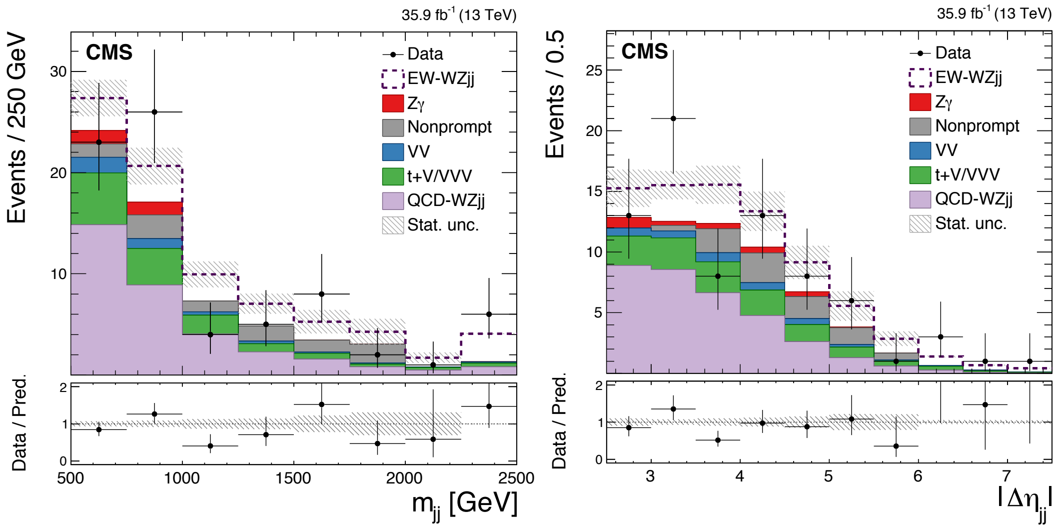

Figure 7: The invariant mass of the two highest p_T jets (left panel) and the rapidity separation (right panel) in a VBS WZ event.

3.3 Search for VBS *ZZ*

The search for VBS *ZZ* [8] production is performed in a final state comprised of two pairs of oppositely charged leptons consistent with the presence of two *Z*-boson candidates. The largest background is the QCD induced production of the same process. This makes it crucial to use a machine learning technique to separate the signal from the background. A multi-variate analysis (MVA) is constructed where the input variables include lepton kinematic and angular variables. The distribution of the M_{jj} and η_{jj}, relevant for VBS topologies, is shown in Fig. 8. This process has not been observed yet, but it is likely that an evidence can be claimed with with full Run II dataset, given that the current observed (predicted) significance is at 2.7 σ (1.6 σ).

4. Rare SM processes

The large dataset collected at the LHC allows for the exploration of rare processes predicted by the SM. The investigation of these processes, in addition to being a robust test of the SM, also facilitates the search for new physics in unexplored event topologies. The search for rare processes such as triboson production and double-parton scattering are discussed in Sec. 4.1 and 4.2 respectively.

4.1 Search for triboson production

The search for triboson production [12] is geared toward the WWW process (shown in the Feynman diagram on the left panel of Fig. 9) that has a production cross section of 0.5 pb (this includes the Higgs mediated channel). However, it is extremely challenging to unearth the WWW

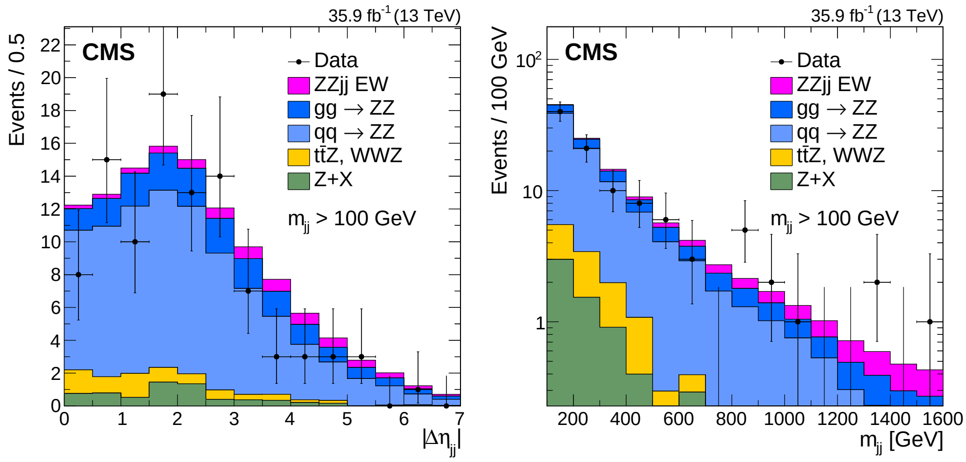

Figure 8: The invariant mass of the two highest p_T jets (left panel) and the rapidity separation (right panel) in a VBS *ZZ* event.

process since the backgrounds associated even with same-signed and trileptonic channels is high. Unlike the VBS signature, a smoking gun signal does not exist for triboson event topologies. The search is carried out in nine bins (shown on the right panel of Fig. 9), where the same-signed channel accounts for six bins (channels are split by lepton flavor and whether the *W* boson is consistent with an on-shell decay) and the trilepton channel accounts for three bins based on the number of OSSF leptons. The observed (expected) sensitivity of the analysis is 0.6 (1.78) σ.

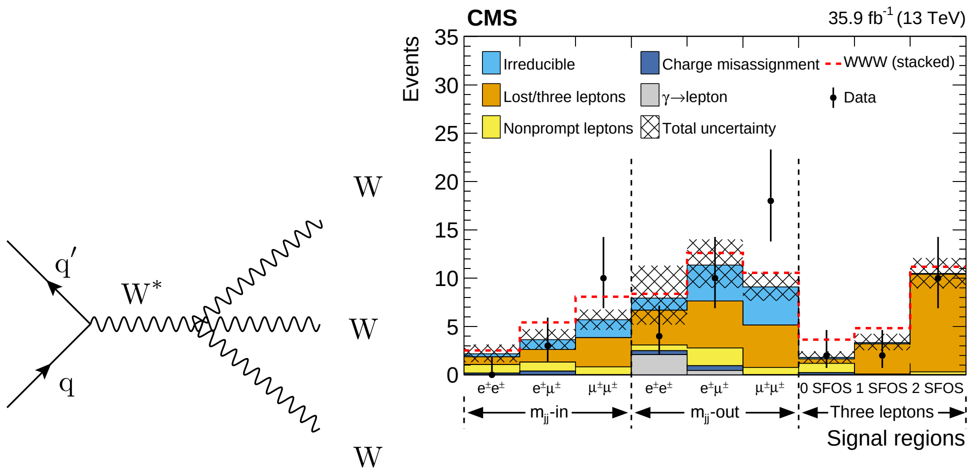

Figure 9: Left panel: The Feynman diagram associated with WWW production. Right panel: The expected and observed event yields in nine channels that were designed based on the maximal discrimination of signal with respect to the background processes.

4.2 Double-parton scattering

Double parton scattering [13] refers to the occurrence of two parton-parton interactions in one proton-proton (p-p) collision. The cross section is factorized into two single hard scattering processes:

$$\sigma_{\mathrm{AB}}^{\mathrm{DPS}} = \frac{n}{2}\frac{\sigma_A \sigma_B}{\sigma_{eff}} \tag{4.1}$$

where n is set to 2 for distinguishable processes and σ_{eff} is a function of the parton distribution in the transverse plane. The production of two W-bosons in an event is explored as this can be used to study WW scattering. A cartoon of the process is shown on the right panel of Fig. 10. The leptonic decays of the W-boson are used to isolate the signal. A multivariate discriminator is designed to distinguished between WZ and non-prompt leptons. The discriminator is constructed with eleven kinematic and angular leptonic variables, the output of which can be seen on the left panel of Fig. 10. This lead to the first evidence of double parton scattering with a significance of 3.9 σ.

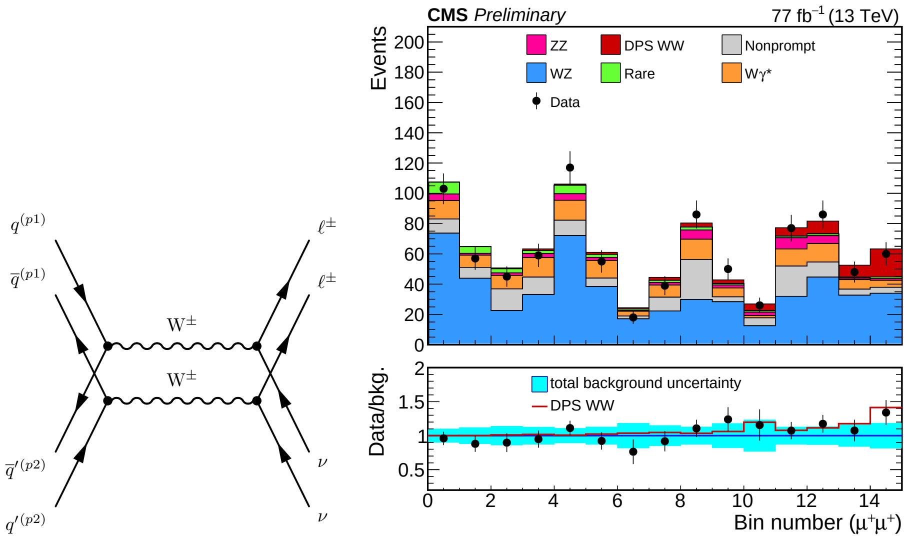

Figure 10: Left panel: Cartoon of the double parton scattering process. Right panel: The output of the multivariate analysis in one of the signal regions, comprised on identically charged muon events. The bin numbers refer to signal regions constructed on two-dimensional multivariate distributions designed to discriminate the signal from prompt (WZ) and non-prompt (misidentified) leptons.

5. Search for anomalous trilinear and quartic couplings

At low energies, the SM Lagrangian can be extended by the Operator Product Expansion

$$\mathscr{L} = \mathscr{L}_{\mathrm{SM}} + \sum_i \frac{c_i}{\Lambda^2}\mathscr{O}_i + \sum_j \frac{f_j}{\Lambda^4}\mathscr{O}_j + \cdots \tag{5.1}$$

where $\mathscr{O}$ represents the higher order, dim-6 and dim-8, operators with coefficients c_i and f_j that are multiplicative factors to these operators respectively. In Eq. 5.1, Λ is the scale of new physics and for $\Lambda \to \infty$, $\mathscr{L} = \mathscr{L}_{\mathrm{SM}}$. The operators $\mathscr{O}$ are constructed out of SM fields and respect gauge invariance. The coefficients are typically incorporated as free parameters which allow for the search for heavy new physics in a model independent way. The search for trilinear ands quartic couplings is discussed in Sections 5.1 and 5.2 respectively.

5.1 Search for anomalous trilinear couplings

The following CP-conserving dimension-6 operators are included in the non-SM part of the Lagrangian:

$$\mathscr{O}_{\mathrm{WWW}} = Tr\left[W_{\mu\nu}W^{\nu\rho}W^{\mu}_{\rho}\right]$$
$$\mathscr{O}_{\mathrm{B}} = (D_{\mu}\Phi)^{\dagger}B^{\mu\nu}(D_{\nu}\Phi)$$
$$\mathscr{O}_{\mathrm{W}} = (D_{\mu}\Phi)^{\dagger}W^{\mu\nu}(D_{\nu}\Phi)$$

The search for anomalous trilinear couplings is carried out in diboson (WW and WZ) final states [14]. Since the analysis is geared toward finding anomalous contributions to the SM, whose effects are pronounced at high $\hat{s}$, jet substructure techniques are particularly well suited to study its impact. The hadronic W or Z candidate is an anti-k_T8 (anti-k_T jet reconstructed with a cone of $\Delta R < 0.8$) jet with $p_T > 200$ GeV. The probability of a jet being consistent with a two-prong decay (n-subjettiness or τ_2/τ_1) is required to be 0.6. The pruned mass of the jet lies between 65-105 GeV. The distribution of the soft drop mass can be seen in Fig. 11, where the sidebands demarcated with vertical lines is used to determine the backgrounds in the signal region. The use of advanced analysis techniques renders this analysis the most sensitive study of anomalous trilinear couplings.

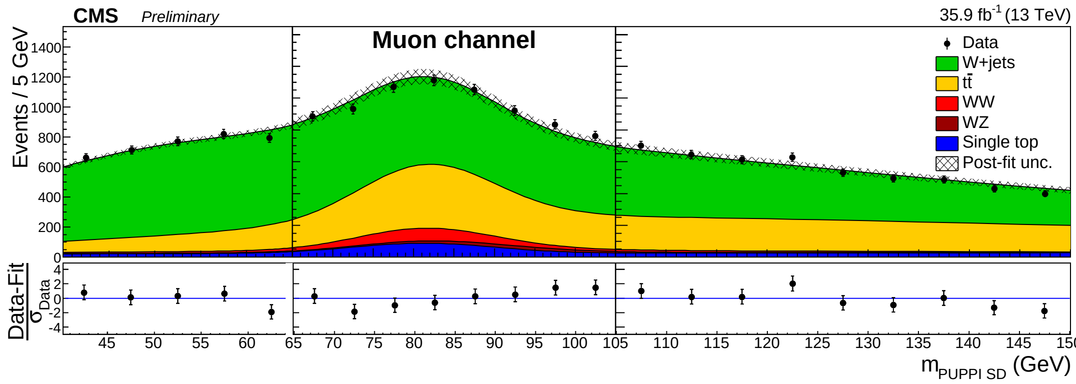

Figure 11: The mass of the jet reconstructed with the soft-drop algorithm in the muon channel. The backgrounds are determined from the sidebands of the distribution demarcated here with vertical lines.

5.2 Search for anomalous quartic couplings

The following CP-conserving quartic terms are included in the non-SM part of the Lagrangian in a search for anomalous quartic couplings. The relevance of these operators for specific vertices is shown in Table 1.

$$\begin{aligned}
\mathscr{O}_{\mathrm{S},0} &= \left[(D_{\mu}\Phi)^{\dagger}D_{\nu}\Phi\right]\times\left[(D_{\mu}\Phi)^{\dagger}D_{\nu}\Phi\right]\\
\mathscr{O}_{\mathrm{S},1} &= \left[(D_{\mu}\Phi)^{\dagger}D^{\mu}\Phi\right]\times\left[(D_{\nu}\Phi)^{\dagger}D^{\nu}\Phi\right]\\
\mathscr{O}_{\mathrm{M},0} &= Tr\left[\hat{W}_{\mu\nu}\hat{W}^{\mu\nu}\right]\times\left[(D_{\beta}\Phi)^{\dagger}D^{\beta}\Phi\right]\\
\mathscr{O}_{\mathrm{M},1} &= Tr\left[\hat{W}_{\mu\nu}\hat{W}^{\nu\beta}\right]\times\left[(D_{\beta}\Phi)^{\dagger}D^{\mu}\Phi\right]\\
\mathscr{O}_{\mathrm{M},6} &= \left[(D_{\mu}\Phi)^{\dagger}\hat{W}_{\beta\nu}\hat{W}^{\beta\nu}D^{\mu}\Phi\right]
\end{aligned}$$

Relevant operator	Vertex		
	WWWW	WWZZ	ZZZZ
$\mathcal{O}_{S,0}, \mathcal{O}_{S,1}$	✓	✓	✓
$\mathcal{O}_{M,0}, \mathcal{O}_{M,1}, \mathcal{O}_{M,6}, \mathcal{O}_{M,7}$	✓	✓	✓
$\mathcal{O}_{M,2}, \mathcal{O}_{M,3}, \mathcal{O}_{M,4}, \mathcal{O}_{M,5}$	0	✓	✓
$\mathcal{O}_{T,0}, \mathcal{O}_{T,1}, \mathcal{O}_{T,2}$	✓	✓	✓
$\mathcal{O}_{T,5}, \mathcal{O}_{T,6}, \mathcal{O}_{T,7}$	0	✓	✓
$\mathcal{O}_{T,8}, \mathcal{O}_{T,9}$	0	0	✓

Table 1: The operators relevant for specific vertices.

$$
\begin{aligned}
\mathcal{O}_{M,7} &= \left[(D_\mu \Phi)^\dagger \hat{W}_{\beta\nu} \hat{W}^{\beta\mu} D^\nu \Phi \right] \\
\mathcal{O}_{T,0} &= Tr\left[W_{\mu\nu} W^{\mu\nu}\right] \times Tr\left[W_{\alpha\beta} W^{\alpha\beta}\right] \\
\mathcal{O}_{T,1} &= Tr\left[W_{\alpha\nu} W^{\mu\beta}\right] \times Tr\left[W_{\mu\beta} W^{\alpha\nu}\right] \\
\mathcal{O}_{T,2} &= Tr\left[W_{\alpha\mu} W^{\mu\beta}\right] \times Tr\left[W_{\beta\nu} W^{\nu\alpha}\right]
\end{aligned} \tag{5.2}
$$

As in the case of trilinear couplings, the search for quartic couplings [15] is focussed on the exploration of the the high $\hat{s}$ region of phase space where the impact of these operators is expected to be more pronounced. The VBS topology is exploited by placing requirements on M_{jj} and the Zeppenfeld variable, while using additional jet substructure techniques to "tag" W or Z jet to set the most stringent limits on the Wilson coefficients. The distribution of the invariant mass of the WW or the WZ system can be seen on the left panel of Fig. 12. The summary of Wilson coefficients associated with the $\mathcal{O}_T$ operators is shown on the right panel of Fig. 12.

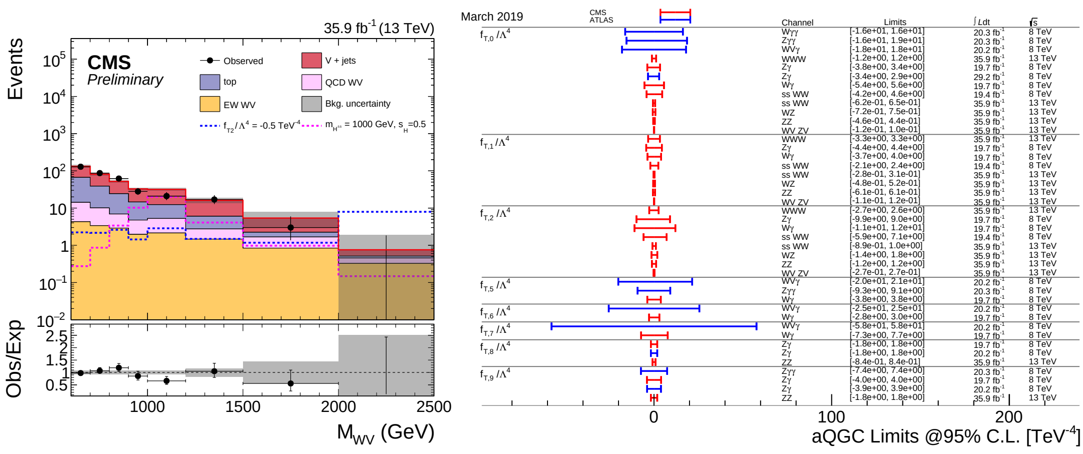

Figure 12: Left panel: The invariant mass of the WW or the WZ system with the corresponding enhancements obtained by the anomalous contributions to the SM. Right panel: The summary of the limits on the Wilson coeffcient f_T parameters associated with the $\mathcal{O}_T$ as described in the array of equations described in Eqn. 5.2.

6. Conclusion

This document presents a compendium of results relevant to multiboson physics. This area of study is expected to gain further momentum as Run III of the LHC commences.

References

[1] CMS Collaboration, Measurement of the WW cross section pp collisions at $\sqrt{s}$=13 TeV, CMS-PAS-SMP-16-006, https://cds.cern.ch/record/2160868

[2] C. Oleari, Loops and Legs in Quantum Field Theory, http://www.sciencedirect.com/science/article/pii/S0920563210001994

[3] B´ahr, M., Gieseke, S., Gigg, M.A. et al. Eur. Phys. J. C (2008) 58: 639. https://doi.org/10.1140/epjc/s10052-008-0798-9

[4] CMS Collaboration, Measurements of the pp $\rightarrow$ WZ inclusive and differential production cross sections and constraints on charged anomalous triple gauge couplings at $\sqrt{s}$= 13 TeV", Journal of High Energy Physics, 2019, 10.1007/JHEP04(2019)122, https://doi.org/10.1007/JHEP04(2019)122

[5] CMS Collaboration, Measurement of the pp $\rightarrow$ ZZ production cross section at $\sqrt{s} = 13$ TeV with the Run 2 data set, CMS-PAS-SMP-19-001, https://cds.cern.ch/record/2668717

[6] CMS Collaboration, Observation of Electroweak Production of Same-Sign W Boson Pairs in the Two Jet and Two Same-Sign Lepton Final State in Proton-Proton Collisions at $\sqrt{s} = 13$ TeV, Phys. Rev. Lett., https://link.aps.org/doi/10.1103/PhysRevLett.120.081801

[7] CMS Collaboration, Measurement of electroweak WZ boson production and search for new physics in WZ + two jets events in pp collisions at $\sqrt{s} = 13$ TeV, Phys. Lett. B, 10.1016/j.physletb.2019.05.042

[8] CMS Collaboration, Measurement of vector boson scattering and constraints on anomalous quartic couplings from events with four leptons and two jets in proton–proton collisions at s=13 TeV, Phys. Lett. B, 10.1016/j.physletb.2017.10.020

[9] CMS Collaboration, Measurement of differential cross sections for Z boson pair production in association with jets at $\sqrt{s} = 8$ and 13 TeV, Phys. Lett. B, 10.1016/j.physletb.2018.11.007

[10] CMS Collaboration, Search for anomalous triple gauge couplings in WW and WZ production in lepton + jet events in proton-proton collisions at $\sqrt{s} = 13$ TeV", CMS-SMP-18-008, https://cds.cern.ch/record/2683318

[11] CMS Collaboration, Search for anomalous electroweak production of vector boson pairs in association with two jets in proton-proton collisions at 13 TeV, Phys. Lett. B, 10.3204/PUBDB-2019-02650

[12] CMS Collaboration, Search for the production of $W^{\pm}W^{\pm}W^{\mp}$ events at $\sqrt{s} = 13$ TeV, Phys. Rev. D, 10.3204/PUBDB-2019-02651

[13] CMS Collaboration, Evidence for WW production from double-parton interactions in proton-proton collisions at $\sqrt{s} = 13$ TeV, https://cds.cern.ch/record/2689470

[14] CMS Collaboration, Search for anomalous triple gauge couplings in WW and WZ production in lepton + jet events in proton-proton collisions at $\sqrt{s} = 13$ TeV, arXiv:1907.08354

[15] CMS Collaboration, Search for anomalous electroweak production of vector boson pairs in association with two jets in proton-proton collisions at 13 TeV, Phys. Lett. B, 798, 134985. 37 p, May, 2019, arXiv:1905.07445, doi: 10.3204/PUBDB-2019-02650

PoS(ALPS2019)055